

Journal Pre-proofs

acMultivariate geostatistical analysis of stable isotopes in Portuguese varietal extra virgin olive oils

Nicasio T. Jiménez-Morillo, Vera Palma, Raquel Garcia, José Alberto Pereira, Cristina Barrocas Dias, Maria João Cabrita

PII: S0026-265X(20)30698-6
DOI: <https://doi.org/10.1016/j.microc.2020.105044>
Reference: MICROC 105044

To appear in: *Microchemical Journal*

Received Date: 2 March 2020
Revised Date: 14 April 2020
Accepted Date: 15 May 2020

Please cite this article as: N.T. Jiménez-Morillo, V. Palma, R. Garcia, J. Alberto Pereira, C. Barrocas Dias, M. João Cabrita, acMultivariate geostatistical analysis of stable isotopes in Portuguese varietal extra virgin olive oils, *Microchemical Journal* (2020), doi: <https://doi.org/10.1016/j.microc.2020.105044>

This is a PDF file of an article that has undergone enhancements after acceptance, such as the addition of a cover page and metadata, and formatting for readability, but it is not yet the definitive version of record. This version will undergo additional copyediting, typesetting and review before it is published in its final form, but we are providing this version to give early visibility of the article. Please note that, during the production process, errors may be discovered which could affect the content, and all legal disclaimers that apply to the journal pertain.

© 2020 Published by Elsevier B.V.



1 **Multivariate geostatistical analysis of stable isotopes in Portuguese varietal extra**
2 **virgin olive oils**

3

4 Nicasio T. Jiménez-Morillo^{a,b}, Vera Palma^b, Raquel Garcia^a, José Alberto Pereira^c,

5 Cristina Barrocas Dias^{b,d}, Maria João Cabrita^{a,e,*}

6

7 ^a MED – Mediterranean Institute for Agriculture, Environment and Development,
8 Universidade de Évora, Pólo da Mitra, Ap. 94, 7006-554 Évora, Portugal

9 ^bHERCULES, Universidade de Évora, Palácio do Vimioso, 7000-089 Évora, Portugal.

10 ^c Centro de Investigação de Montanha (CIMO), ESA, Instituto Politécnico de Bragança,
11 Campus de Santa Apolónia, 5300-253 Bragança, Portugal

12 ^d Departamento de Química, Escola de Ciências e Tecnologia, Universidade de Évora,
13 Rua Romão Ramalho, 59, 7000 Évora, Portugal

14 ^e Departamento de Fitotecnia, Escola de Ciências e Tecnologia, Universidade de Évora,
15 Núcleo da Mitra, Ap. 94, 7006-554 Évora, Portugal.

16 *mjbc@uevora.pt

17

18 **Abstract**

19 Stable isotope contents of carbon, hydrogen and oxygen are known to reflect the geo-
20 climatic conditions under which olives grown. This study aims to unravel the correlation
21 between some of the main geographic variables and the isotopic composition of different
22 Portuguese varietal extra virgin olive oil (EVOO) samples. Thus, the isotopic
23 composition ($\delta^{13}\text{C}$, $\delta^{18}\text{O}$ and $\delta^2\text{H}$) of 38 EVOO samples from 11 olive varieties from 2
24 Portuguese regions (Alentejo and Trás-os-Montes) was studied using an elemental
25 analyzer coupled to an isotope ratio mass spectrometry. Multivariate analysis indicated
26 that bulk $\delta^{13}\text{C}$, $\delta^2\text{H}$ and $\delta^{18}\text{O}$ values were enough to significantly ($P < 0.05$) predict
27 altitude, latitude, longitude, temperature, rainfall, and sea distance. This work showed
28 that the assessment of EVOO isotopic composition give information not only on the
29 geographic origin, but also on the environmental conditions. To the best of our
30 knowledge, this is the first report on bulk isotopic composition of Portuguese EVOOs.

31

32

33 **Keywords:** Extra virgin olive oil, Geographic origin, Multi linear regression, Stable
34 isotopes, Statistical analysis

35

36 1. Introduction

37 Olive oil is unique among other vegetable oils owing to the health benefits, nutritional
38 properties and peculiar organoleptic characteristics. Since they are only mechanically
39 extracted and consumed without any further refining process, the natural compounds are
40 preserved contributing to its higher nutritional value [1]. Recent studies have described
41 potential health benefits to some compounds that compose olive oil matrix, being
42 considered as a functional food, which arouses a huge interest for its consumption [2].
43 Extra virgin olive oil (EVOO) is considered the top grade of olive oil, and with the
44 commercial value of EVOO and the recent introduction on the market of high-quality
45 monovarietal olive oils, it can lead to an increase of fraudulent practices, namely those
46 related with the botanical and geographical origin of the olive oil [3]. Therefore, an
47 especial attention has been given to EVOO authenticity, particularly on ascertain its
48 geographic and varietal origin. The noticeable influence that geoclimatic conditions have
49 on the organoleptic quality of olive oils [4], prompted the attempt to differentiate EVOO
50 based on their geographic origin using suitable analytical methodologies. EVOO
51 geographic denomination is not determined by the commonly used physico-chemical
52 parameters [5] since they are not sufficiently accurate to enable this differentiation.
53 Therefore, it is an imperative need the development of appropriate analytical tools
54 combined with statistical methods to guarantee the authenticity and traceability of olive
55 oils, preventing illicit practices and protecting both the producers and consumers.
56 Nowadays, the evaluation of the stable isotope composition of the main bioelements (C,
57 N, H and O) by isotope ratio mass spectrometry (IRMS) seems to be a powerful approach
58 to ensure geographical origin of foodstuffs [6]. Stable isotope analysis of fatty acids was
59 introduced in the 1970s to study the pathways of lipid biosynthesis [7], but it was recently
60 that IRMS technique has been applied to the authentication of olive oils. Since stable

61 isotopes can provide valuable information of geoclimatic characteristics of the production
62 areas, as well as of the agricultural practices [8], they can be used as key markers of
63 geographical origin, becoming a valuable approach in such kind of studies. Particularly,
64 the C isotope composition ($\delta^{13}\text{C}$) of plant components (fruits, roots, leaves, etc.) is mainly
65 related to the type of photosystem (C_3 and C_4), as well as to several environmental and
66 edaphic factors, like humidity, temperature, precipitation, salinity of soil, water stress,
67 etc. [9]. On the other hand, the isotopic composition of H and O are indicators of the water
68 uptake and evapotranspiration of the growing plant, which, in turn, are very sensitive to
69 the geoclimatic conditions (latitude, longitude, altitude, temperature, etc.) of production
70 areas [10, 11]. Furthermore, $\delta^2\text{H}$ and $\delta^{18}\text{O}$ values are determined by the possible
71 fractionation associated with the plant tissues biosynthesis pathways [12]. Owing to the
72 conspicuous complexity of the data obtained with the different isotope analysis
73 techniques, the use of multivariate statistical analyses, such as Principal Component
74 Analysis (PCA), Partial Least Squares regression, Multi Linear Regression (MLR) and
75 Discriminant Analysis, for both the interpretation of these data and the determination of
76 geographical origin of olive oils [13,14] is needed.

77 This study aimed to evaluate the suitability of stable isotope composition of the main
78 bioelements (C, H and O) for discriminating Portuguese varietal EVOO samples
79 according to their geoclimatic conditions using multivariate statistical methods, such as
80 PCA and MLR, for data evaluation.

81 **2. Materials and Methods**

82 **2.1. Samples and experimental design**

83 A total of 38 well-catalogued EVOO (*Olea europaea* L.) samples from 11 different olive
84 varieties (Arbequina, Blanqueta, Carrasquenha, Cobrançosa, Cordovil de Serpa, Galega

85 Vulgar, Madural, Verdeal, Negrinha do Freixo, Picual and Verdeal Alentejana) produced
86 in 12 different locations belonging to two well-differentiate Portuguese regions, Alentejo
87 (Elvas, Mourão, Vidigueira, Serpa, Évora, Ferreira do Alentejo) and Trás-os-Montes
88 (Freixo de Espada à Cinta, Alfandega da Fé, Macedo de Cavaleiros, Mirandela, Valpaços,
89 and Vila Flor) (26 and 12 olive oil samples, respectively), were collected in November
90 and December of 2016. For most of the samples, approximately 5 kg of each olive
91 varieties were processed separately in an Abencor® system within 24 hours from
92 harvesting. Fruits were crushed with a hammer mill and the olive paste was malaxed at
93 25° C for 30 min, in an olive paste mixer, finally the olive oil was separated by
94 centrifugation. Other samples were taken directly from olive oil mills to avoid possible
95 undeclared mixtures with olive oils from other cultivars and geographical origins before
96 bottling. They were stored in dark-brown glass bottles at 20°C in the dark. Each EVOO
97 sample was geo-referenced, with data of latitude (UTM), longitude (UTM), altitude (m
98 a.s.l.), sea distance (km), mean annual temperature (°C) and mean annual rainfall (mm)
99 respectively assigned (Table 1).

100 **2.4. Stable isotope analysis**

101 The carbon, hydrogen and oxygen isotope composition ratios ($^{13}\text{C}/^{12}\text{C}$, $^2\text{H}/^1\text{H}$ and
102 $^{18}\text{O}/^{16}\text{O}$, respectively) of EVOO samples were determined by elemental analysis/isotope
103 ratio mass spectrometry (EA/IRMS). The EA/IRMS system consisted of a Flash 2000 HT
104 elemental analyzer (Thermo Scientific, Bremen, Germany) with two reactors: i)
105 Combustion (C, N and S), and ii) Pyrolysis (H and O). The elemental analyzer is coupled
106 by a ConFlo IV (Thermo Scientific) continuous flow open split interface to a Delta V
107 Advantage isotope ratio mass spectrometer (Thermo Scientific). Carbon isotope analysis
108 used helium as carrier gas at a flow rate of 80 mL/min, while for hydrogen isotope
109 analysis the helium flow was set at 120 mL/min. EVOO samples (0.5 to 1 mg) were

110 weighed in cups (IVA Analysentechnik GmbH & Co. KG, Meerbusch, Germany) made
111 of tin for carbon and of silver for hydrogen and oxygen analysis. The cups were closed,
112 folded, pressed to a small size and loaded in a MAS 200R (Thermo Scientific) automatic
113 sampling carousel. Appropriate calibration standards were prepared in the same manner
114 and placed within batches of samples.

115 For carbon isotope analysis the cups were flush-combusted and flush-reduced
116 concurrently under a helium carrier steam and oxygen pulse at 1020 °C in a quartz reactor
117 filled with chromium oxide (Cr_2O_3), silvered cobaltous-cobaltic oxide ($\text{Ag}(\text{Co}_3\text{O}_4)$) and
118 reduced copper (Cu). The gases were dried through a 10 cm long glass column filled with
119 anhydrous magnesium perchlorate ($\text{Mg}(\text{ClO}_4)_2$), and then directed through a 3 m long
120 and 4 mm i.d. stainless steel gas chromatography column packed with Porapak stationary
121 phase at 40 °C for the separation of CO_2 , which was analysed for its isotopic composition
122 in the Delta V Advantage isotope ratio mass spectrometer. Pure CO_2 gas was inserted into
123 the He carrier flow as pulses of the reference gas (250 mL/min).

124 For hydrogen and oxygen isotope ratios the samples were analysed using the pyrolysis
125 reactor. This consists of an outer ceramic (Al_2O_3) tube and an inner glassy carbon reactor
126 tube filled with high-purity glassy carbon granulates, and wool of silver and quartz. The
127 silver cups were dropped sequentially under a steam of helium into the reactor tube held
128 at 1450 °C. The produced pyrolysis gasses were passed through a 10 cm long glass
129 column filled with a mixture of anhydrous magnesium perchlorate ($\text{Mg}(\text{ClO}_4)_2$), to dry
130 the gas, and Carbosorb, to trap CO_2 generated during the pyrolysis reaction. The dry
131 pyrolysis gasses were directed through a 3 m long and 4 mm i.d. stainless steel gas
132 chromatography column packed with Porapak stationary phase at 70 °C for the
133 separation of H_2 and CO. Hydrogen and oxygen were analysed for its isotopic

134 composition on the Delta V Advantage isotope ratio mass spectrometer. Pure H₂ and CO
 135 gas were inserted into the He carrier flow as pulses of the reference gas (250 mL/min).

136 The stable isotope abundances are reported in the delta (δ) notation ($\delta^{13}\text{C}$, $\delta^2\text{H}$ and $\delta^{18}\text{O}$)
 137 in variations relative to an international standard. The isotope value was defined by
 138 Coplen in 2011 [15], according to equation 1:

139

$$140 \quad \delta^i E_{\text{sample}} = \frac{R(iE/jE)_{\text{sample}}}{R(iE/jE)_{\text{standard}}} - 1 \quad 1)$$

141

142 Where “R” is the molar ratio of the heavy (iE) to light (jE) most abundant isotope of
 143 chemical element “E” ($^{13}\text{C}/^{12}\text{C}$, $^2\text{H}/^1\text{H}$ and $^{18}\text{O}/^{16}\text{O}$). The “ δ ” values are reported in
 144 milliurey (mUr). The stable isotope standard for carbon is the Vienna Pee Dee Belemnite
 145 limestone (VPDB), while for hydrogen and oxygen is the Vienna Standard Mean Ocean
 146 Water (VSMOW). The standards used were those recognized by the International Atomic
 147 Energy Agency (IAEA). The standard deviation of bulk $\delta^{13}\text{C}$, $\delta^2\text{H}$ and $\delta^{18}\text{O}$ were ± 0.1 ,
 148 1.0 and 0.5 mUr, respectively. Each sample was measured in duplicated ($n=2$) to obtain
 149 its average and standard deviation.

150 **2.5. Statistical analysis**

151 Multivariate data treatments were carried out with the software Statgraphics Centurion
 152 XV, using the stable isotope values of carbon, hydrogen and oxygen of EVOO samples
 153 ($n= 38$) as independent variables. Principal component analysis (PCA) was used for
 154 simultaneous ordination of different geographic and climatic dependent variables and the
 155 $\delta^{13}\text{C}$, $\delta^2\text{H}$ and $\delta^{18}\text{O}$ values (independent variables), illustrating their mutual relationships.
 156 Multiple linear regression (MLR) was applied considering the stable isotope composition

157 as independent variables and the geographic and climatic factors as dependent variables.
158 Spurious models due to overfitting were detected and discarded after repeating MLR
159 models with fully randomized dependent variables. This work has not used training
160 models. Because, to our knowledge, this is the first study in which the isotope
161 compositions of the Portuguese EVOOs are determined. Therefore, no previous data were
162 available to evaluate training models. In addition, the predictions were made directly from
163 all the experimental data acquired in this study, validating the predicted values by means
164 of the leave-on-out, cross-validation method.

165

166 **3. Results and Discussion**

167 **3.1. Stable isotope analysis of EVOO samples**

168 The $\delta^{13}\text{C}$ values (Figure 1A) of EVOO samples, both from Alentejo and Trás-os-Montes
169 regions, displayed a typical behavior of plants with C_3 photosystem [16]. The ranges of
170 $\delta^{13}\text{C}$ values were different between the two main Portuguese regions, i.e., 3.9 mUr for
171 Alentejo (from -27.9 mUr to -31.8 mUr) and 2.4 mUr for Trás-os-Montes (from -28.1
172 mUr to -30.5 mUr). Nevertheless, their mean values ($\delta^{13}\text{C}_{\text{Alentejo}} = -29.6 \pm 0.6$ mUr,
173 $\delta^{13}\text{C}_{\text{Trás-os-Montes}} = -29.3 \pm 0.6$ mUr) showed no significant differences ($P > 0.05$). Although
174 there was not a significant difference between regions, it was observed a little ^{13}C -
175 enrichment in Trás-os-Montes samples. This fact may be due either to the differences in
176 the carbon isotopic composition between the subregions or to the variations in the olive
177 varieties [17]. In fact, we can observe figure 2 (A and B) that displays the $\delta^{13}\text{C}$ values of
178 EVOO samples both for different subregions and olive varieties. With respect to
179 subregions, it is observed that EVOO samples cultivated in Vila Flor (Trás-os-Montes)
180 were isotopically heavier than the rest one, while Ferreira do Alentejo (Alentejo) olive

181 oils showed the lowest $\delta^{13}\text{C}$ value. The $\delta^{13}\text{C}$ values of plant cultured under irrigation
182 proceedings display a more negative value (^{13}C -depletion) than that cultivated under
183 drought conditions [18]. This idea may be related to the isotopic value of EVOO from
184 Ferreira do Alentejo. However, we do not have this information. Concerning the varieties,
185 Picual, collected in Alentejo, was isotopically lighter than the rest of varieties.
186 Cobrançosa variety presents similar isotopic C values either in Alentejo or Trás-os-
187 Montes. Therefore, the little difference in carbon composition between these regions
188 seems to be mainly related to the location of the olive tree cultivations and/or agricultural
189 procedures (irrigation).

190 Similarly, to carbon isotope composition, the mean $\delta^{18}\text{O}$ value (Alentejo = 23.0 ± 0.7
191 mUr and Trás-os-Montes = 22.7 ± 0.7 mUr) showed no significant difference ($P > 0.05$)
192 between the two regions studied (Fig. 1B). However, their ranges of values were different,
193 i.e., 3.2 mUr for Alentejo (from 24.5 to 21.3 mUr) and 2.1 for Trás-os-Montes (from 23.5
194 to 21.4 mUr). This difference may be linked with the subregion and/or olive variety. In
195 this case, the fact that EVOO samples cultivated in Trás-os-Montes show a $\delta^{18}\text{O}$ value
196 slightly lighter than that in Alentejo (Fig. 1B) may be due to the fact that the EVOOs
197 produced in Valpaços, Macedo de Cavaleiros and Mirandela (Trás-os-Montes) displayed
198 a lighter isotopic composition of oxygen than the others (Fig. 2C). On the other hand,
199 some olive varieties cultivated in Alentejo showed an isotopic composition heavier than
200 that were cultivated in Trás-os-Montes (Fig. 2D and Table 1).

201 On the other hand, the mean $\delta^2\text{H}$ value of the two regions of Portugal ($\delta^2\text{H}_{\text{Alentejo}} = -137.2$
202 ± 2.2 mUr, $\delta^2\text{H}_{\text{Trás-os-Montes}} = -149.3 \pm 2.8$ mUr) showed significant difference ($P < 0.05$),
203 being Trás-os-Montes region more ^2H -depleted than Alentejo one ($\delta^2\text{H}_{\text{Trás-os-Montes}}$: from
204 -152.3 to -148.4 mUr, $\delta^2\text{H}_{\text{Alentejo}}$: from -146.6 to -130.7 mUr). The ^2H composition, which
205 reflects the type of water uptake by the plants during its growth, is highly linked

(negatively and/or positively) both to the climatic conditions of the production area, as well as to its geographical characteristics [19]. In our case, Trás-os-Montes region shows higher elevation and rainfall amount than Alentejo one (Table 1). Nevertheless, Trás-os-Montes shows low seasonal temperatures (Table 1). The combination of low rainfall amount and high temperature causes a high evapotranspiration of the plants [20, 21], which is translated in an increase in the elimination of the light hydrogen isotope. Therefore, EVOO samples from Alentejo showed a heavier hydrogen composition. This result was also observed when it is studied the $\delta^2\text{H}$ value of the different subregions (Fig. 2E, Table 1), since the EVOO samples cultivated in subregions located into Trás-os-Montes were isotopically lighter than that are cultivated in subregions of Alentejo. Concerning olive varieties, there are significant difference among varieties (Fig. 2F). However, this difference may be directly related to culture location, because all olive varieties cultivated in Trás-os-Montes regions (Cobrançosa, Madural, Negrinha do Freixo and Verdeal) showed lower ^2H composition than that cultured in Alentejo. For instance, the Cobrançosa variety is present in both regions; however, those cultivated in Trás-os-Montes showed a significant ^2H -depletion compared with those from Alentejo. This may support the idea that the culture location is directly related to the isotopic value.

3.2. Chemometric analysis

Principal components analysis (PCA) was used to identify the possible positive and inverse correlation (angle of 0° or 180° , respectively) between the stable isotope (carbon, hydrogen and oxygen) values and geographical and climatic variables (Figure 3). Up to 75% of the total variance can be explained by two first components (component 1: 55.52 % and component 2: 20.41 %). The scatterplot of the loadings of PC-1 vs PC-2 showed that $\delta^2\text{H}$ values were strongly positive correlated with climatic conditions, mainly temperature (0°), as well as the geographic longitude of the production area. Nevertheless,

231 these are inversely correlated (180°) with latitude, altitude and, rainfall. With respect to
232 sea distance, $\delta^2\text{H}$ values showed no correlation (90°). Several researchers observed the
233 same trend between hydrogen isotope and environmental factors. For example,
234 Chiocchini et al., in 2016 [22] found that high altitude produced the ^2H -depletion of
235 organic samples. The positive correlation with temperature has recently been observed by
236 Jiménez-Morillo et al. [23] using pyrolysis compound-specific isotope analysis. With
237 respect to carbon isotope, it is highly correlated with sea distance (close to 0°) of the
238 production area. However, the correlation with its altitude and latitude was not strong
239 (higher than 45°). and rainfall. Furthermore, $\delta^{13}\text{C}$ values were negatively correlated with
240 longitude (180°). These correlations were also established by Camin et al. in 2010 [24].
241 The temperature and rainfall were not correlated (90°) with the carbon isotope
242 composition of the EVOO samples. Oxygen isotope composition of EVOO samples was
243 directly correlated with longitude (close to 0°) but inversely with sea distance (180°). This
244 correlation was also observed by other researchers [21, 25, 26], who observed that oxygen
245 was linked with longitude (UTM) and distance from the sea (km). These correlations were
246 corroborated using multi linear regression (MLR). The MLR, exclusively using the stable
247 isotope values (independent variables) of EVOO samples ($n= 38$) led to significant ($P <$
248 0.05) forecasting models for all geoclimatic (dependent) variables (i.e., latitude,
249 longitude, altitude, rainfall, temperature and sea distance) from the total analysed
250 samples. Fig. 4 plots the observed vs predicted values of each models: a) latitude, b)
251 longitude, c) altitude, d) rainfall, e) temperature, and f) sea distance. The model validation
252 was confirmed by a strict criterion based on the comparing the MLR cross-validation tests
253 (observed vs predicted) with the alternative model computed from the fully randomized
254 latent variables (latitude, longitude, altitude, rainfall, temperature and sea distance) from
255 the 38 EVOO samples studied in this work. These models displayed a poor correlation (P

256 > 0.05) with isotopic data (Figure S1 in supplementary information). Therefore, it is
 257 proved that a significant forecasting model is only possible with the real (experimental)
 258 values [23, 27, 28]. The MLR analysis of $\delta^{13}\text{C}$, $\delta^2\text{H}$ and $\delta^{18}\text{O}$ values of different EVOO
 259 samples allowed to obtain the equations 2-7 of the prediction model:

$$260 \quad \underline{\text{Latitude}} = 23.63 + 0.36 \times \delta^{13}\text{C} - 0.17 \times \delta^2\text{H} \quad 2)$$

$$261 \quad \underline{\text{Longitude}} = 1.37 - 0.24 \times \delta^{13}\text{C} + 0.02 \times \delta^2\text{H} + 0.07 \times \delta^{18}\text{O} \quad 3)$$

$$262 \quad \underline{\text{Altitude}} = 423.61 + 61.70 \times \delta^{13}\text{C} - 11.96 \times \delta^2\text{H} \quad 4)$$

$$263 \quad \underline{\text{Rainfall}} = -2948.33 - 26.65 \times \delta^2\text{H} \quad 5)$$

$$264 \quad \underline{\text{Temperature}} = 69.42 + 0.32 \times \delta^2\text{H} - 0.33 \times \delta^{18}\text{O} \quad 6)$$

$$265 \quad \underline{\text{Sea distance}} = 1335.06 + 29.78 \times \delta^{13}\text{C} - 14.18 \times \delta^{18}\text{O} \quad 7)$$

266 Only those independent variables whose value of P has been less than 0.05 have been
 267 taken into account for the creation of the models. Therefore, there are geoclimatic
 268 variables that displayed in their model one or two independent variables (stable isotope
 269 composition).

270 The existence of correlation ($P < 0.05$) between stable isotope values and dependent
 271 variables (climatic and geographical) may explain why there was a significant difference
 272 between two Portuguese regions. On the other hand, it could say that the combined use
 273 of ^2H , ^{13}C and ^{18}O isotopic composition gives a valuable and precise information for the
 274 assessing of geographic origin of Portuguese EVOO samples, which is a very powerful
 275 tool, which could help to fight against food-fraud suffered by EVOO sector in Portugal.
 276 As far as authors are aware, this work is the first one that use, in combination, bulk
 277 isotopic composition ($\delta^2\text{H}$, $\delta^{13}\text{C}$ and $\delta^{18}\text{O}$) and multivariate statistical analysis (PCA and
 278 MLR), to assess the geographic origin of Portuguese EVOOs.

279

280 **Abbreviations Used**

281 C, carbon; DA, discriminant analysis; EA, elemental analysis; EVOO, extra virgin olive
282 oil; H, hydrogen; IAEA, international atomic energy agency; IRMS, isotope ratio mass
283 spectrometry; MLR, multi linear regression; N, nitrogen; O, oxygen; PCA, principal
284 component analysis; VPDB, Vienna pee dee belemnite; VSMOW, Vienna standard
285 mean ocean water.

286

287 **Acknowledgments**

288 This work was funded by European Regional Development Fund (FEDER) and National
289 Funds through Foundation for Science and Technology (FCT) under Project “Por3O -
290 Portuguese Olive Oil Omics for traceability and authenticity -
291 PTDC/AGRPRO/2003/2014, and by National Funds through FCT - Foundation for
292 Science and Technology under the Projects UIDB/05183/2020 and UID/AGR/00690/2019.
293 Pedro N. Jiménez-Morillo is acknowledged for statistical assistance.

294 **References**

- 295 [1] Campestre, C, Angelini, G., Gasbarri, C. & Angerosa, F. (2017). The Compounds
296 Responsible for the Sensory Profile in Monovarietal Virgin Olive Oils. *Molecules*, 22,
297 1833. <https://doi.org/10.3390/molecules22111833>
- 298 [2] Ray, N.B., Hilsabeck, K.D., Karagiannis, T.C., & McCord, D.E. (2019) Chapter 36 -
299 Bioactive Olive Oil Polyphenols in the Promotion of Health. In *The Role of Functional*
300 *Food Security in Global Health* (pp 623–663). Singh, R.B.; Watson, R.R.; Takahashi, T.,
301 Eds; Academy Press Cambridge, Massachusetts

- 302 [3] Garcia, R., Martins, N. & Cabrita, M.J. (2013). Putative markers of adulteration of
303 extra virgin olive oil with refined olive oil: Prospects and limitations. *Food Research*
304 *International*, 54, 2039–2044. <https://doi.org/10.1016/j.foodres.2013.05.008>.
- 305 [4] Abu-Reidah, I.M., Yasin, M., Urbani, S., Sevili, M. & Montedoro, G. (2013). Study
306 and characterization of Palestinian monovarietal Nabali virgine olive oils from northern
307 west Bank of Palestine, *Food Research International*, 54, 1959–1964.
308 <https://doi.org/10.1016/j.foodres.2013.09.004>.
- 309 [5] Aparicio, R., Morales, M.T., Aparicio-Ruiz, R., Tena, N. & García-González, D.L.
310 (2013). Authenticity of olive oil: Mapping and comparing official methods and promising
311 alternatives, *Food Research International*, 54, 2025–2038.
312 <https://doi.org/10.1016/j.foodres.2013.07.039>.
- 313 [6] Camin, F., Boner, M., Bontempo, L., Fauhl-Hassek, C., Kelly, S.D., Riedl, J. &
314 Rossmann, A. (2017). Stable isotope techniques for verifying the declared geographical
315 origin of food in legal cases, *Trends in Food Science & Technology*, 61, 176–187.
316 <https://doi.org/10.1016/j.tifs.2016.12.007>.
- 317 [7] De Niro, M.J., & Epstein, S. (1977). Mechanism of Carbon Isotope Fractionation
318 Associated with Lipid Synthesis, *Science*, 197, 261–263.
- 319 [8] Styring, A. K., Ater, M., Hmimsa, Y., Fraser, R., Miller, H., Neef, R., Pearson, J.A.
320 & Bogaard, A. (2016). Disentangling the effect of farming practice from aridity on crop
321 stable isotope values: A present-day model from Morocco and its application to early
322 farming sites in the eastern Mediterranean. *The Anthropocene Review*, 3, 2–22.
323 <https://doi.org/10.1177/2053019616630762>.

- 324 [9] Hartman, G. & Danin, A. (2010). Isotopic values of plants in relation to water
325 availability in the Eastern Mediterranean region, *Oecologia*, 162, 837–852.
326 <https://doi.org/10.1007/s00442-009-1514-7>.
- 327 [10] Brooks, R.J., Barnard, H.R., Coulombe, R. & McDonnell, J.J. (2010). Ecohydrologic
328 separation of water between trees and streams in a Mediterranean climate, *Nature*
329 *Geoscience*, 3, 100–104. <https://doi.org/10.1038/ngeo722>.
- 330 [11] Kelly, S.D. & Rhodes, C. (2002). Emerging techniques in vegetable oil analysis
331 using stable isotope ratio mass spectrometry, *Grasas y Aceites*, 53, 34–44.
332 <https://doi.org/10.3989/gya.2002.v53.i1.28>.
- 333 [12] Schmidt, H.L., Werner, R.A. & Eisenreich, W. (2003). Systematics of ^2H patterns in
334 natural compounds and its importance for the elucidation of biosynthetic pathways.
335 *Phytochemistry Reviews*, 2, 61–85.
336 <https://doi.org/10.1023/B:PHYT.0000004185.92648.ae>.
- 337 [13] Gómez-Caravaca, A.M., Maggio, R.M. & Cerretani, L. (2016). Chemometric
338 applications to assess quality and critical parameters of virgin and extra-virgin olive oil.
339 A review, *Analytica Chimica Acta*, 913, 1–21. <https://doi.org/10.1016/j.aca.2016.01.025>.
- 340 [14] Kritiotti, A., Menexes, G. & Drouza, C. (2018). Chemometric characterization of
341 virgin olive oils of the two major Cypriot cultivars based on their fatty acid composition,
342 *Food Research International*, 103, 426–437.
343 <https://doi.org/10.1016/j.foodres.2017.10.064>.
- 344 [15] Coplen, T.B. (2011). Guidelines and recommended terms of expression of stable-
345 isotope-ratio and gas-ratio measurement results. *Rapid Communications in Mass*
346 *Spectrometry*, 25, 2538–2560. <https://doi.org/10.1002/rcm.5129>.

- 347 [16] Spangenberg, J.E. (2016). Bulk C, H, O, and fatty acid C stable isotope analyses for
348 purity assessment of vegetable oils from the southern and northern hemispheres, *Rapid*
349 *Communications in Mass Spectrometry*, 30, 2447–2461.
350 <https://doi.org/10.1002/rcm.7734>.
- 351 [17] Bianchi, G., Angerosa, F., Camera, L., Reniero, F. & Anglani, C. (1993). Stable
352 carbon isotope ratios (carbon-13/carbon-12) of olive oil components. *Journal of*
353 *Agricultural and Food Chemistry*, 41, 1936–1940. <https://doi.org/10.1021/jf00035a024>.
- 354 [18] Aramendía, M.A., Marinas, A., Marinas, J.M., Sánchez, E., Urbano, F.J., Guillou,
355 C., Moreno Rojas, J.M., Moalem, M. & Rallo, L. (2010). A nuclear magnetic resonance
356 (^1H and ^{13}C) and isotope ratio mass spectrometry ($\delta^{13}\text{C}$, $\delta^2\text{H}$ and $\delta^{18}\text{O}$) study of
357 Andalusian olive oils. *Rapid Communications in Mass Spectrometry*, 24, 1457–1466.
358 <https://doi.org/10.1002/rcm.4538>.
- 359 [19] Bontempo, L., Camin, F., Larcher, R., Nicolini, G., Perini, M. & Rossmann, A.
360 (2009) Coast and year effect on H, O and C stable isotope ratios of Tyrrhenian and
361 Adriatic Italian olive oils. *Rapid Communications in Mass Spectrometry*, 23, 1043–1048.
362 <https://doi.org/10.1002/rcm.3968>.
- 363 [20] Kaseke, K.F., Wang, L., Wanke, H., Turewicz, V. & Koeniger, P. (2016) An
364 Analysis of Precipitation Isotope Distributions across Namibia Using Historical Data.
365 *PLoS ONE*, 11: e0154598. <https://doi.org/10.1371/journal.pone.0154598>.
- 366 [21] Clark, I. & Fritz, P. (1997) *Environmental Isotopes in Hydrogeology*. Lewis
367 Publishers, Boca Raton, New York, pp. 328.
- 368 [22] Chiocchini, F., Portarena, S., Ciolfi, M., Brugnoli, E. & Lauteri, M. (2016). Isoscapes
369 of carbon and oxygen stable isotope compositions in tracing authenticity and

- 370 geographical origin of Italian extra-virgin olive oils, *Food Chemistry*, 202, 291–301.
371 <https://doi.org/10.1016/j.foodchem.2016.01.146>.
- 372 [23] Jiménez-Morillo, N.T., Cabrita, M.J., Barrocas-Dias, C., González-Vila, F.J.,
373 González-Pérez, J.A. (2020). Pyrolysis-compound-specific hydrogen isotope analysis
374 ($\delta^2\text{H}$ Py-CSIA) of Mediterranean olive oils. *Food Control*, 110, 107023.
375 <https://doi.org/10.1016/j.foodcont.2019.107023>.
- 376 [24] Camin, F., Larcher, R., Perini, M., Bontempo, L., Bertoldi, D., Gagliano, G.,
377 Nicolini, G. & Versini, G. (2010). Characterisation of authentic Italian extra-virgin olive
378 oils by stable isotope ratios of C, O and H and mineral composition, *Food Chemistry*,
379 118, 901–909. <https://doi.org/10.1016/j.foodchem.2008.04.059>.
- 380 [25] Feng, X. & Epstein, S. (1995). Carbon isotopes of trees from arid environments and
381 implications for reconstructing atmospheric CO_2 concentration. *Geochimica et*
382 *Cosmochimica Acta*, 59, 2599–2608. [https://doi.org/10.1016/0016-7037\(95\)00152-2](https://doi.org/10.1016/0016-7037(95)00152-2).
- 383 [26] Peng, T.R., Chen, K.Y., Zhan, W.J., Lu, W.C. & Tong, L.T.J. (2015). Use of stable
384 water isotopes to identify hydrological processes of meteoric water in montane
385 catchments. *Hydrological Processes*, 29, 4957–4967. <https://doi.org/10.1002/hyp.10557>.
- 386 [27] De la Rosa, J.M., Jiménez-González, M.A., Jiménez-Morillo, N.T., Knicker, H.,
387 Almendros, G. (2019). Quantitative forecasting black (pyrogenic) carbon in soils by
388 chemometric analysis of infrared spectra. *Journal of Environmental Management*, 251,
389 109567. <https://doi.org/10.1016/j.jenvman.2019.109567>.
- 390 [28] Jiménez-González, M.A., Álvarez, A.M., Carral, P., Almendros, G. (2019).
391 Chemometric assessment of soil organic matter storage and quality from humic acid
392 infrared spectra. *Science of the Total Environment*, 685, 1160–1168.
393 <https://doi.org/10.1016/j.scitotenv.2019.06.231>.

394

395 **Conflict of Interest**

396

397 **In the name of all my co-workers I declare that there is no conflict of**
398 **interest.**

399

400 **Maria Joao Cabrita**

401

402 Nicasio T. Jiménez-Morillo – Methodology, Formal analysis, Investigation, Writing original draft

403

404 Vera Palma - Investigation

405

406 Raquel Garcia – Investigation, Sampling

407

408 José Alberto Pereira – Investigation, Sampling

409

410 Cristina Barrocas Dias – Investigation, Writing – review & editing

411 Maria João Cabrita – Conceptualization, resources, writing – review & editing, Supervision, Project
412 administration

413

414 **Highlights:**

415

416 - Isotopic composition ($\delta^{13}\text{C}$, $\delta^{18}\text{O}$ and $\delta^2\text{H}$) of Portuguese varietal olive oils

417 - Bulk $\delta^{13}\text{C}$, $\delta^2\text{H}$ and $\delta^{18}\text{O}$ values can be used to predict geographic variables

418 - Extra virgin olive oils from Alentejo and Trás-os-Montes

419 - First report on bulk isotopic composition of Portuguese EVOOs

420

421 **Figure captions**

422 Figure 1. Boxplots of the bulk carbon ($\delta^{13}\text{C}_{\text{bulk}}$ values, A), oxygen ($\delta^{18}\text{O}_{\text{bulk}}$ values, B) and
423 hydrogen ($\delta^2\text{H}_{\text{bulk}}$ values, C) isotope composition of two Portuguese region (Alentejo and Trás-
424 os-Montes). Boxplots display the ranges, lower and upper quartiles (Q1, Q3), and the median
425 (Q2).

426 Figure 2. Boxplots of the Portuguese subregions and olive varieties of bulk carbon ($\delta^{13}\text{C}_{\text{bulk}}$
427 values A and B, respectively), oxygen ($\delta^{18}\text{O}_{\text{bulk}}$ values C and D, respectively) and hydrogen
428 ($\delta^2\text{H}_{\text{bulk}}$ values E and F, respectively). Boxplots display the ranges, lower and upper quartiles
429 (Q1, Q3), and the median (Q2).

430 Figure 3. Plot of components weights for the geographical variables and the stable isotope
 431 composition of carbon, hydrogen and oxygen ($\delta^{13}\text{C}$, $\delta^2\text{H}$, $\delta^{18}\text{O}$, respectively) of EVOO samples.

432 Fig 4. Observed vs. predicted values for geographical and climatic variables: A) latitude, B)
 433 longitude, C) altitude, D) rainfall, E) temperature, and F) Sea distance, calculated by PLS
 434 regression using stable isotope values of EVOOs as predictors.

435

436

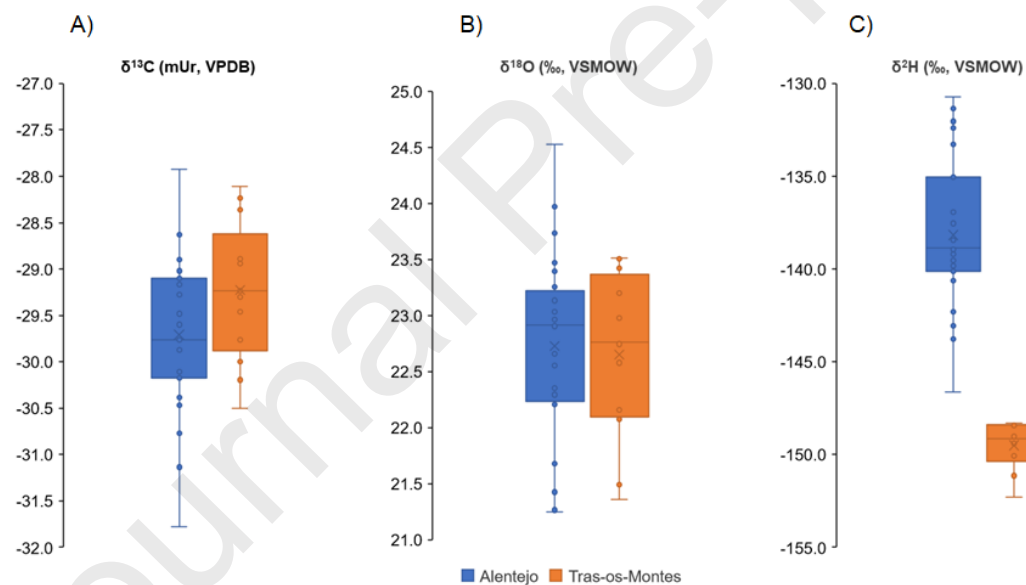
437 Table 1. Varieties, origin, region, geo-climatic information and stable isotope
 438 composition of EVOO samples.

Code	Varieties	Origen	Re gio n *	Latit ude (UT M)	Longi tude (UT M)	Altitu de (m.a.s. l)	Rai nfal l (m m)	Tempe rature (°C)	Sea distance (km)	$\delta^{13}\text{C}$ (mUr, VPDB)	$\delta^2\text{H}$ (mUr, VSMOW)	$\delta^{18}\text{O}$ (mUr, VSMO W)
AArb 1	Arbequina	Elvas	AL	38.88	7.16	328	679. 3	18.01	197.1	-29.6	-139.8	17.9
AArb 3	Arbequina	Évora	AL	38.41	7.72	190	738. 1	18.17	96.27	-29.2	-132.4	22.3
AArb 4	Arbequina	Vidigueira	AL	38.17	7.72	163	679. 3	18.01	92.76	-29.9	-138.2	22.7
AArb 5	Arbequina	Ferreira do Alentejo	AL	38.06	8.11	140	679. 3	17.6	61.99	-31.1	-138.2	23.5
ABla 1	Blanqueta	Elvas	AL	38.88	7.16	328	679. 3	18.01	197.1	-27.9	-132.3	23.3
ACar 1	Carrasquenh a	Elvas	AL	38.88	7.16	328	679. 3	17.6	197.1	-30.1	-130.7	24.5
ACob 1	Cobrançosa	Vidigueira	AL	38.17	7.72	163	679. 3	17.6	92.76	-29.8	-138.5	23.7
ACob 3	Cobrançosa	Ferreira do Alentejo	AL	38.06	8.11	140	679. 3	18.01	61.99	-30.8	-137.5	23.0
ACob 4	Cobrançosa	Vidigueira	AL	38.17	7.72	163	738. 1	18.17	92.76	-30.4	-138.9	23.0
ACob 5	Cobrançosa	Elvas	AL	38.88	7.16	328	625. 3	18.41	197.1	-29.0	-142.3	23.4
ACob 6	Cobrançosa	Vidigueira	AL	38.17	7.72	163	738. 1	18.17	92.76	-29.5	-131.3	25.5
ACob 7	Cobrançosa	Évora	AL	38.41	7.72	190	679. 3	17.99	96.27	-29.1	-136.9	22.9
ACob 8	Cobrançosa	Elvas	AL	38.88	7.16	328	679. 3	17.6	197.1	-28.6	-143.8	22.2
ACor 1	Cordovil de Serpa	Elvas	AL	38.88	7.16	328	679. 3	17.6	197.1	-29.1	-143.0	22.9
ACor 2	Cordovil de Serpa	Vidigueira	AL	38.17	7.72	163	679. 3	17.6	92.76	-30.2	-140.0	22.3
ACor 3	Cordovil de Serpa	Ferreira do Alentejo	AL	38.06	8.11	140	679. 3	17.6	61.99	-30.2	-139.2	22.9
ACor 4	Cordovil de Serpa	Serpa	AL	37.94	7.60	218	679. 3	17.6	114.17	-29.1	-138.9	24.0
AGal 1	Galega Vulgar	Ferreira do Alentejo	AL	38.06	8.11	140	679. 3	18.01	61.99	-29.8	-132.0	25.9
AGal 2	Galega Vulgar	Mourão	AL	38.36	7.29	186	679. 3	18.01	132.69	-29.1	-133.3	22.4
AGal 4	Galega Vulgar	Elvas	AL	38.88	7.16	328	738. 1	18.17	197.1	-28.9	-135.1	23.1
AMad 1	Madural	Elvas	AL	38.88	7.16	328	679. 3	17.6	197.1	-29.9	-137.5	21.3
APic 1	Picual	Elvas	AL	38.88	7.16	328	679. 3	17.6	197.1	-30.5	-146.6	21.7
APic 3	Picual	Évora	AL	38.41	7.72	190	679. 3	17.6	96.27	-30.4	-139.5	22.2
APic 4	Picual	Vidigueira	AL	38.17	7.72	163	679. 3	18.01	92.76	-30.1	-140.6	22.9
APic 5	Picual	Ferreira do Alentejo	AL	38.06	8.11	140	679. 3	18.01	61.99	-31.8	-140.1	21.4

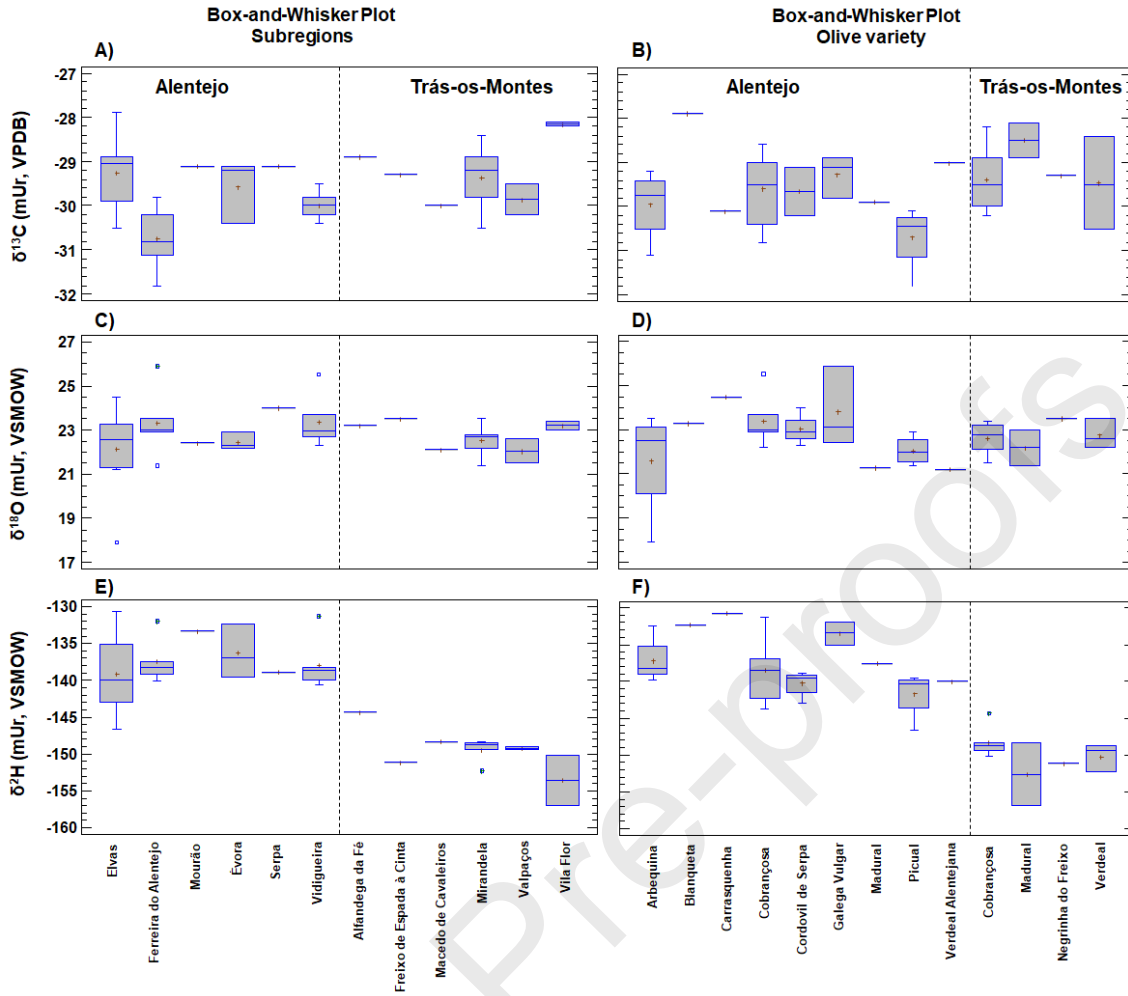
AVer 1	Verdeal Alentejana	Elvas	AL	38.88	7.16	328	738.1	18.17	197.1	-29.0	-140.0	21.2
TM Cob 1	Cobrançosa	Macedo de Cavaleiros	TM	41.53	6.95	655	865.4	12.56	153.56	-30.0	-148.3	22.1
Cob 2	Cobrançosa	Mirandela	TM	41.48	7.18	254	121.25	12.75	134.78	-29.2	-149.3	22.8
Cob 3	Cobrançosa	Alfandega da Fé	TM	41.34	6.96	549	865.4	13.58	150.71	-28.9	-144.3	23.2
Cob 4	Cobrançosa	Mirandela	TM	41.49	7.26	359	121.25	12.75	127.3	-29.8	-148.4	22.7
Cob 6	Cobrançosa	Valpaços	TM	41.61	7.31	428	121.25	12.75	126.27	-30.2	-149.0	21.5
Cob 7	Cobrançosa	Vila Flor	TM	41.31	7.15	550	121.25	12.51	133.27	-28.2	-150.1	23.4
Mad 1	Madural	Vila Flor	TM	41.30	7.16	555	121.25	12.75	133.27	-28.1	-156.9	23.0
Mad 2	Madural	Mirandela	TM	41.49	7.18	228	121.25	12.75	134.78	-28.9	-148.3	21.4
Neg 3	Negrinha do Freixo	Freixo de Espada à Cinta	TM	41.11	6.84	605	121.25	12.51	153.63	-29.3	-151.1	23.5
Ver 1	Verdeal	Mirandela	TM	41.49	7.26	349	121.25	12.75	127.3	-28.4	-148.8	23.5
Ver 2	Verdeal	Valpaços	TM	41.61	7.30	416	865.4	13.58	126.27	-29.5	-149.4	22.6
Ver 3	Verdeal	Mirandela	TM	41.49	7.17	234	121.25	12.75	134.78	-30.5	-152.3	22.2

439 * AL = Alentejo; TM = Trás-os-Montes

440

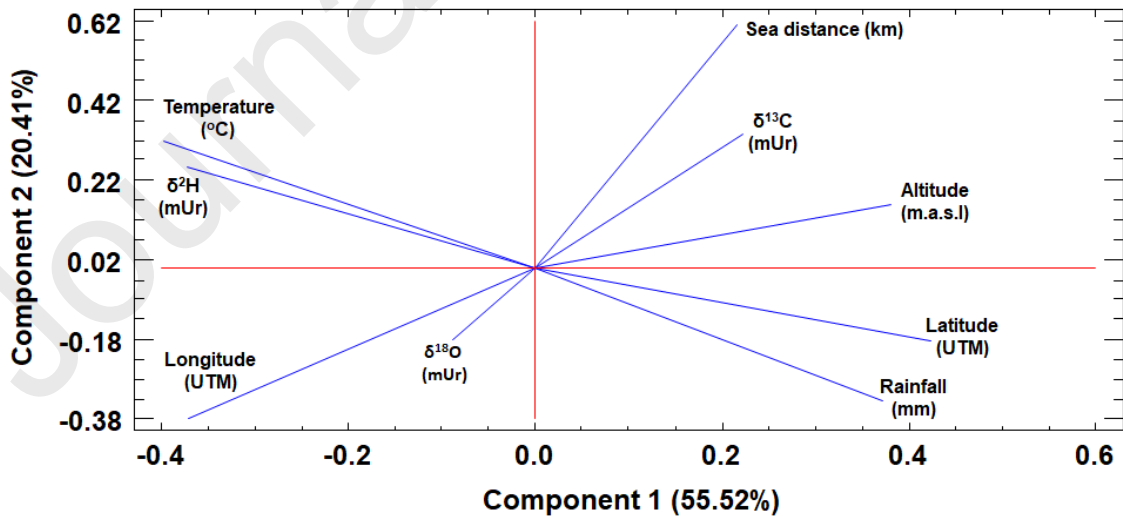


441

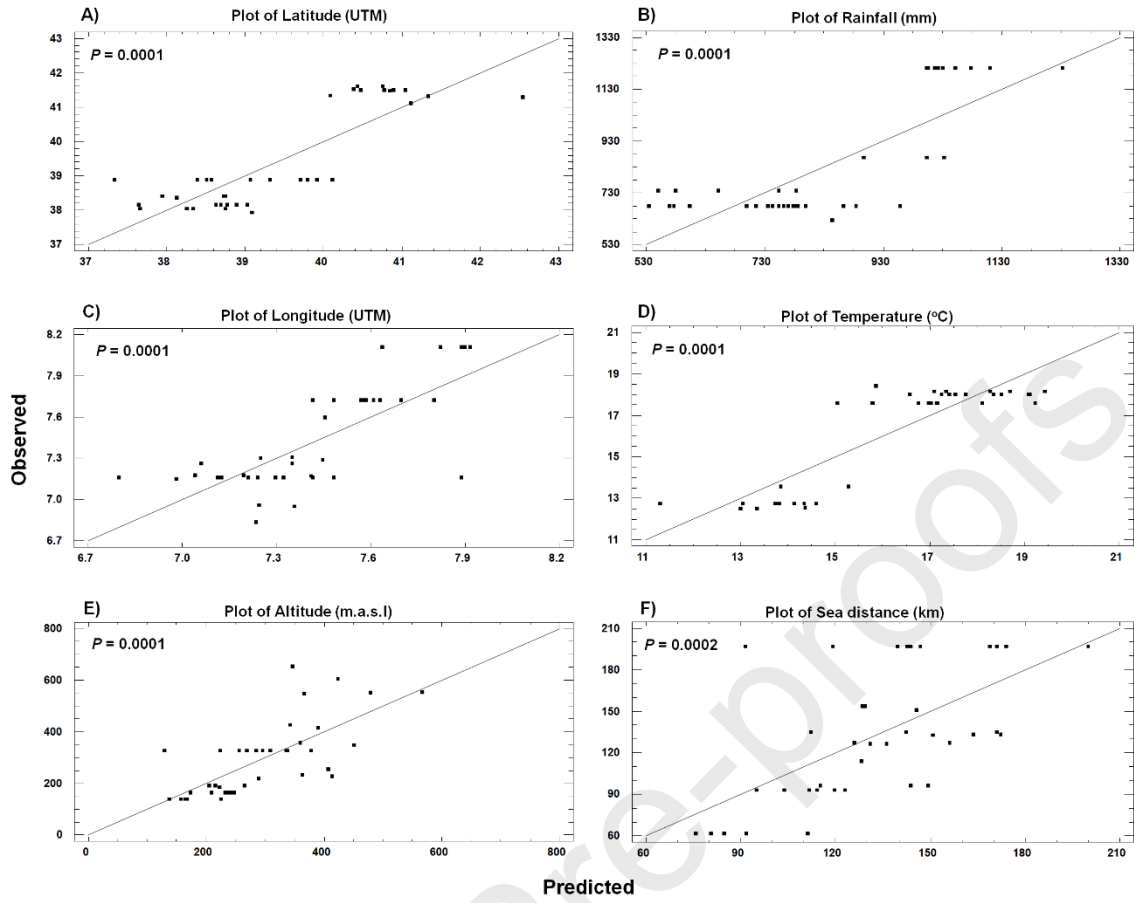


442

Plot of Component Weights



443



444